地震研究所彙報
Bull. Earthq. Res. Inst.
Univ. Tokyo
Vol. 76 (2001) pp. 377-389

Transportation of H_2O and Melting beneath the Japan Arcs

Hikaru Iwamori*

Department of Earth and Planetary Sciences, University of Tokyo

Abstract

Recent knowledge concerning the phase relationships of hydrous peridotitic and basaltic systems allows us to model fluid generation and migration in subduction zones. Here I present: (1) numerical models for the transportation of H_2O and melting beneath the Japanese islands, in which generation and migration of aqueous fluid, its interaction with the convecting solid, and melting are considered, based on the phase relationships; (2) predictions of the corresponding seismic structures based on the calculated distribution of the fluids (aqueous fluids and melts); (3) 3-D seismic tomographic images beneath the islands; (4) analyses of the distribution of the volcanoes and the volcanic chains; and (5) comparisons between the model predictions and the observations. The model calculation suggests that in northeast Japan, nearly all of the H_2O expelled from the subducted Pacific plate is hosted by serpentine and chlorite just above the plate, and is brought down to ~150 km. Breakdown of serpentine and chlorite at these depths results in the formation of a fluid column through which H_2O is transported upwards, and results in the initiation of melting in the mantle wedge beneath the backarc. Seismic tomographic studies suggest the existence of such a melting region beneath the backarc. In central Japan, the subducted Philippine Sea plate overlaps the subducted Pacific plate. This geometry causes slow thermal recovery of the subducted Pacific plate, resulting in dehydration reactions at levels (200–300 km) deeper than in northeast Japan, and deflection of the volcanic chain towards the backarc side. In contrast, in southwest Japan, where a relatively hot part of the Philippine sea plate (Shikoku basin) subducts, the dehydration reactions are predicted to occur at relatively shallow levels (< 100 km in depth). The seismic tomographic image supports well the predicted distribution of the fluids beneath the volcanic front to the forearc region. These comparisons between the model predictions and the observations suggest that the thermal structure (determined by age and subduction velocity) of the subducting plate strongly controls the distribution of the aqueous fluids and melts in subduction zones through the position of the dehydration reactions.

Key words: H_2O, melt, subduction, Japan arcs

1. Introduction

Material recycling in subduction zones, including generation and migration of aqueous fluids and melts, is the key to understanding the origin of volcanism and seismicity in subduction zones. It is also important for understanding the global mass budget, such as formation and growth of the continents, and recycling of volatile components. For example, H_2O brought down greatly affects the viscosity of the mantle, which then affects the convective motion of the mantle and the global balance of mass and energy.

Within the subducting plate, pressure and temperature increase as the plate subducts, which causes dehydration of H_2O-bearing minerals and generation of aqueous fluid. The aqueous fluid generated is thought to ascend due to buoyancy as a porous flow along the crystal grain boundaries or a channel flow through cracks, resulting in melting in the mantle wedge (Fig. 1). However, the processes of dehydra-

*e-mail: hikaku@esp.s.u-tokyo.ac.jp (3-1, Hongo 7 chome, Bunkyo-ku, Tokyo, 113-0033 Japan)

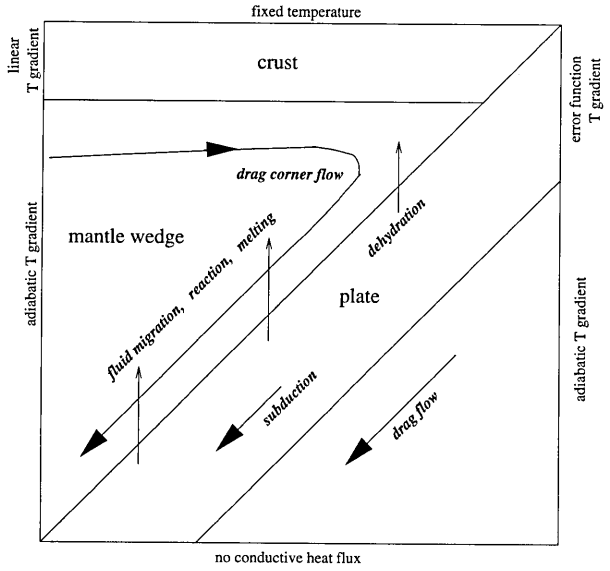

Fig. 1. Schematic figure showing transportation of H_2O and melting in subduction zones. The boundary conditions of temperature for the modelling are shown along the outline of the box.

tion and melting are controlled by many factors, which are poorly constrained at present.

The main aim of this paper is to present models of the fluid processes: generation and migration of H_2O-rich fluid, interactions of the fluid with the convecting solid, and melt generation in this dynamic situation. The model results are compared with the observations such as distribution of volcanoes and seismic structures. The Japan arcs are ideal for this study in terms of variations in subduction parameters (e.g., age of the subducting slab) and the number and the quality of observations. Based on the comparison, it will be shown that the thermal structure of the subducting plate is the main factor controlling the fluid processes. It is noted that this paper involves reviews of the previously published materials, which aims to provide a unified view of the fluid processes in subduction zones.

2. Subduction of plates around the Japan arcs

Two oceanic plates, the Pacific and the Philippine sea plates, subduct beneath the Japan arcs. The Pacific plate subducts at the Kuril trench and the Japan trench beneath Hokkaido, Honshu (northeast and central Japan), and Izu-Ogasawara with the subduction velocity of ~10 cm/yr to the west (e.g., DeMets *et al.*, 1990). The age of the Pacific plate in these regions reaches 130 Ma (Fig. 2). On the other hand, the Philippine sea plate subducts at the Sagami and Nankai trough beneath Honshu (central and southwest Japan), Kyushu, and Ryukyu with subduction velocity of ~3 cm/yr to the northwest (e.g., Seno *et al.*, 1993). The Philippine sea plate can be divided into three regions extending north-south direction, according to the formation age (Fig. 2): (i) the eastern part formed before 40 Ma, including the Izu-Ogasawara arc; (ii) the central part, the Shikoku basin, which was formed as a backarc basin during 27 to 15 Ma (Okino *et al.*, 1994); and (iii) the western part older than 50 Ma, consisting of several old ridges and the basins (e.g., Tokuyama, 1995). The eastern part subducts at the Sagami and the Nankai trough, causing a collision of the Honshu and the Izu-Ogasawara arcs. A former spreading axis exists in the Shikoku basin and subducts at the Nankai trough, between the Kii peninsula and Shikoku. The western part subducts beneath Kyushu and the Ryukyu arc.

The geometry of the subducted Pacific plate is well constrained from the distribution of the hypocenters and the tomographic studies (e.g., Yoshii, 1979; Zhao and Hasegawa, 1993), suggesting that the leading edge reaches a depth of 500 km or more beneath the Japan sea.

The geometry of the subducted Philippine sea plate beneath central Japan has been deduced also from the distribution of the hypocenters and tomographic studies (e.g., Ishida, 1992), suggesting that (i) the leading edge reaches a depth of 60–100 km beneath the northern part of Kanto, central Japan (Fig. 2), overlapping the subducted Pacific plate, and (ii) no subducting plate exists beneath the north of the Izu peninsula, where an arc-arc collision occurs. On the other hand, beneath the western part of central Japan (Tokai region), the leading edge reaches a shallower level of 50–60 km in depth and 36 degrees north in latitude, with a complex geometry probably due to significant deformation of the subducted Philippine sea plate (Yamazaki, 1989).

The subducted Philippine sea plate corresponding to the young Shikoku basin beneath southwest Japan (Shikoku, Chugoku, and northern Kyushu) is also confirmed by the seismicity associated with subduction, which extends over a relatively short distance from the trench, ~150 km in the horizontal distance (the leading edge of the plate with abundant seismicity is located beneath northern Shikoku or

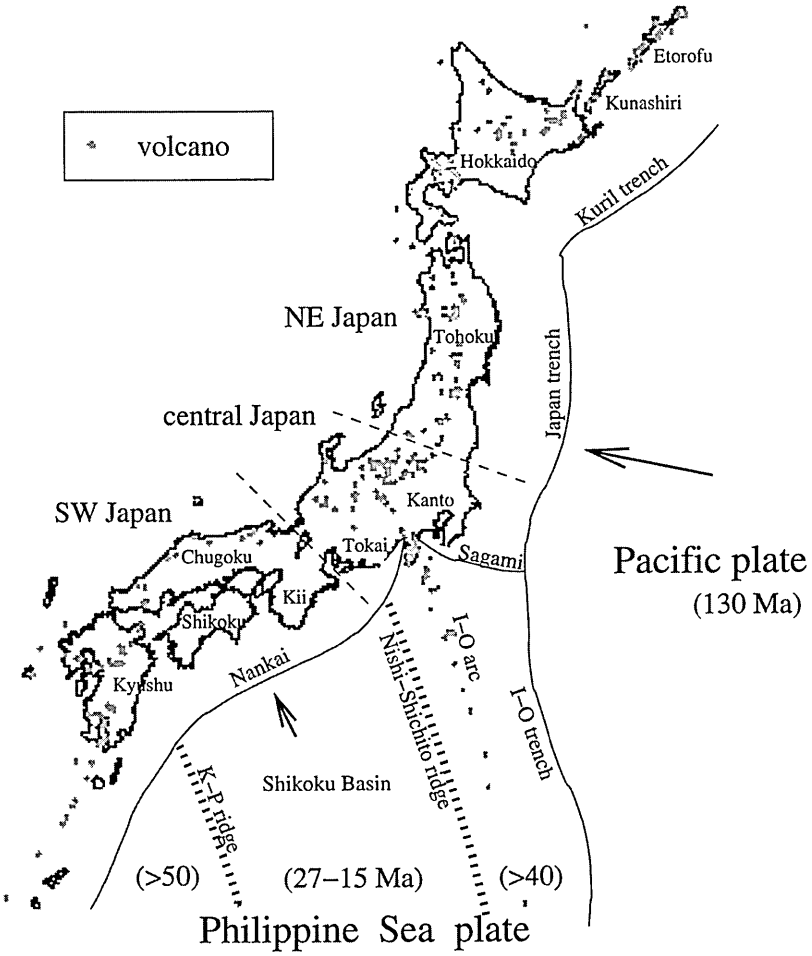

Fig. 2. Location, structure, and age of the plates subducting beneath Japanese islands. I-O arc and I-O trench indicate Izu-Ogasawara arc and trench, respectively. K-P ridge indicates Kyushu-Palau ridge.

Setonaikai). This is explained by quick thermal assimilation of the subducted young Shikoku basin, which becomes aseismic within the short distance. Indeed, an aseismic slab beneath Chugoku (to the north of Setouchi) is suggested, based on the analysis of ScS-wave and its conversion to P-wave (Nakanishi, 1980). The subduction angle is ~15 degrees, possibly reflecting the young buoyant nature of the Shikoku basin, whereas the subducted Philippine sea plate is kinked beneath western Shikoku and northern Kyushu with a steeper subduction angle (~45 degrees) to the west.

In Fig. 2, the Quaternary volcanoes along the Japan arcs are shown by grayish points. The volcanoes are aligned in general parallel to the trenches and the troughs, forming volcanic chains. However, the details of the alignment change along the arcs. For example, along the Kuril arc and in Hokkaido, echelon arrangement of the volcanoes is recognized with Etorofu island, Kunashiri island, and Shiretoko peninsula to Meakan-dake. In northeast Japan, alignment parallel to the trench is recognized along the volcanic front, whereas the volcanoes (between 0 and 14 Ma) on the backarc side form several clusters rather than a continuous chain (Kondo *et al.*, 1998). In central Japan, the parallelism is violated as the volcanic chain significantly deflects towards the backarc side (Iwamori, 2000). In the Chugoku district, southwest Japan, a volcanic zone aligned along the Japan sea coast (Daisen volcanic zone) has been thought to be associated with subduction of the Philippine sea plate. However, Iwamori (1991; 1992) discussed that the Daisen volcanic zone is a product of crustal melting induced by alkaline basaltic volcanism associated with mantle upwelling abundant in volatile and incompatible elements since 12 Ma. A similar alkaline basaltic volcanism of non-island arc type is recognized during the same period over a

wide area, including the backarc side of northern Kyushu (e.g., basalts in Iki island and Kita-Matsuura), Korea and mainland China (Whitford-Stark, 1987). On the other hand, the andesitic volcanism of the island-arc type is recognized from the volcanic front in northern Kyushu to the Ryukyu arc (e.g., Kuju, Aso, and Sakurajima volcanoes), which forms a volcanic chain again parallel to the trench (Nankai and Ryukyu troughs).

The along-arc variations in terms of subduction parameters (velocity, angle, and age of the slab), and nature of seismicity and volcanism described above are produced through various processes: thermal structure of the plate and the mantle wedge, chemical reactions (especially dehydration reaction) and their location, and generation-migration of aqueous fluids and melts (e.g., Iwamori, 1998). In the following, first, the numerical modelling which describes these processes is introduced. Then specific cases for the Japan arcs are discussed based on a comparison between the model results and the observations, including seismic structures and distribution of volcanoes.

3. Model of transportation of H_2O and melting

The model described here involves subduction of a plate, convection of mantle wedge, phase relationship of H_2O-bearing rocks for both subducted oceanic crust (basalt) and mantle wedge (peridotite), generation and migration of aqueous fluid, and its reaction with the convecting solid (including melting). Most previous studies focused on one or two of the aspects listed above. However, understanding the processes in subduction zones requires a model integrating all aspects. Iwamori (1998) proposed such an integrated model, with governing equations for mass and energy conservation, parameterized phase relationships for the H_2O-bearing systems, and some simplification. The simplification involves: (i) convection of solid in the mantle wedge is assumed to be induced by the dragging of the subducting plate, and is assumed to be a steady flow with a constant viscosity (i.e., kinematic model); (ii) the aqueous fluid migrates as a porous flow along the solid grain boundaries, without affecting the solid flow; and (iii) the melt does not separate from the solid from which the melt is formed. Assumption (iii) is unrealistic, and indicates that the model cannot be used for properly discussing the relationship between the distribution of melting region and the volcanoes. However, the model provides constraints on the position at which the aqueous fluid is generated, the amount of fluid generated, transportation path of the fluid, and how it reacts with the mantle wedge to produce hydrous minerals and melts.

The corresponding governing equations are as follows (Iwamori, 1998):

$$\frac{\partial(\rho_i\phi_i)}{\partial t}+\nabla\cdot(\rho_i\phi_i\mathbf{V}_i)=\sum_{j\neq i}\Gamma_{j\to i} \text{ and } \sum_i\sum_{j\neq i}\Gamma_{j\to i}=0\ (i,j,=m,s,a) \tag{1}$$

$$\frac{\partial(\rho_b C_b^{H_2O})}{\partial t}+\sum_i^{m,s,a}\nabla\cdot[\rho_i\phi_i C_i^{H_2O}\mathbf{V}_i]=0 \tag{2}$$

$$\nabla^4\Psi_s=0 \text{ and } \mathbf{V}_s=(u_s,v_s)=\left(\frac{\partial\Psi_s}{\partial z},-\frac{\partial\Psi_s}{\partial x}\right) \tag{3}$$

$$\mathbf{V}_m=\mathbf{V}_s \tag{4}$$

$$\mathbf{V}_a=\mathbf{V}_s-\frac{k_{\phi_a}}{\phi_a\eta_a}[\eta_s\nabla^2\mathbf{V}_s+(1-\phi_a)\Delta\rho_a g\mathbf{z}] \text{ and } k_{\phi_a}=\frac{R^2\phi_a^n}{B} \tag{5}$$

$$\left[\sum_i^{m,s}(\phi_i\rho_i C_P^i)+T\Delta S\frac{(\partial\phi_m\rho_m)}{\partial T}\right]\frac{\partial T}{\partial t}= K\nabla^2T-\sum_i^{m,s}(\phi_i\rho_i C_P^i\mathbf{V}_i\cdot\nabla T-T\phi_i\alpha_i\mathbf{V}_i\cdot\nabla P) -T\Delta S\frac{\partial(\phi_m\rho_m)}{\partial(C_b^{H_2O})}\frac{\partial(C_b^{H_2O})}{\partial t} -T\Delta S\nabla\cdot(\phi_m\rho_m\mathbf{V}_m) \tag{6}$$

where the subscript i indicates a phase (m=melt, s=solid, a=aqueous fluid, b=local bulk system ($m+s+a$)), ρ_i is the density, ϕ_i is the volume fraction, $\mathbf{V}_i$ is the velocity vector, $\Gamma_{j\to i}$ is the rate of phase change from j- to i-phase in weight fraction (e.g., $\Gamma_{s\to m}$ is the melting rate), $C_i^{H_2O}$ is the weight fraction of H_2O in phase i, and t is the time. Equation (2) expresses mass balance of H_2O in the local system, where $C_b^{H_2O}$ is the average concentration of H_2O in the local system. Although, at the pressure and temperature of interest, the aqueous fluid dissolves a significant amount of silicate components, $C_a^{H_2O}$ is set to 1 for simplicity. Equation (3) expresses the flow of solid, where Ψ_s is the stream function, u_s and v_s are the horizontal and vertical components of the velocity. Assumptions (i) to (iii) described earlier in this chapter correspond to (3) and (4). Equation (5) expresses the flow of aqueous fluid as a porous flow, where k_{ϕ_a} is the permeability, η_a is the viscosity of aqueous fluid, η_s is the viscosity of solid, $\Delta\rho_a$ is $\rho_s-\rho_a$, g is the gravitational acceleration, $\mathbf{z}$ is the unit vector along the vertical axis, R is the radius of solid grain, n and B are the constants (n

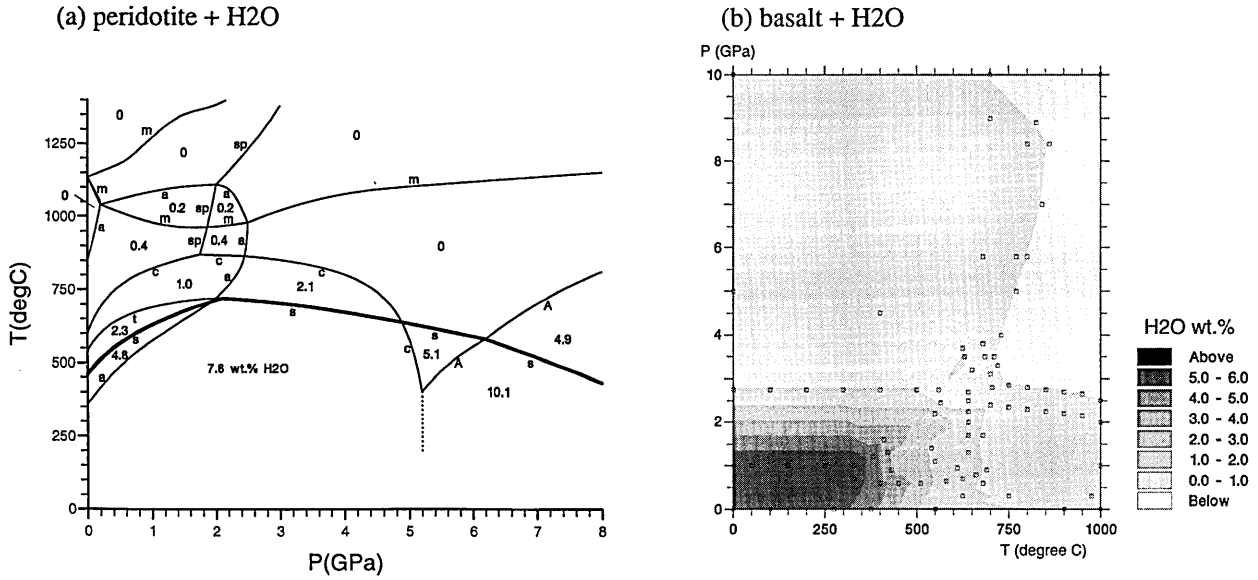

Fig. 3. Maximum content of H_2O in the solid phases (i.e., the maximum $C_s^{H_2O}$) and stability fields of hydrous minerals of (a) peridotite and (b) basalt (after Iwamori (1998)). The letters attached to the stability field boundaries indicate the following mineral phases, which are stable at the side where the letter is attached: a=amphibole; c=chlorite; m=melt; s=serpentine; sp=spinel; t=talc; A=phase A. The maximum $C_s^{H_2O}$ in each region is shown in the central portion of each region.

=3 and $B=10^3$ are assumed (McKenzie, 1984)).

The aqueous fluid is assumed to achieve chemical equilibrium with the surrounding solid during its migration by porous flow. If a channel flow through sparsely distributed cracks occurs, then chemical equilibrium may be violated. A model result incorporating chemical disequilibrium is also presented later in this paper. In either case, the fraction of aqueous fluid is small, and will not affect the flow of solid significantly, which justifies assumption (ii). Equation (6) expresses conservation of energy, where C_i^i is the specific heat at constant pressure, α_i is the thermal expansion coefficient of phase i, ΔS is the entropy change associated with melting, and K is the thermal conductivity. In this equation, energy transportation due to the migration of aqueous fluid and entropy change associated with the generation of aqueous fluid are neglected. Also, local thermal equilibrium, no viscous dissipation of energy, and no entropy change associated with compositional change in each phase are assumed.

To model the generation and the migration of aqueous fluid and melt, phase relationships for the subducting plate and mantle wedge are required. The subducting plate consists of sediment, basaltic oceanic crust, and residual peridotite. The mantle wedge is thought to consist of peridotitic rocks. The H_2O-bearing phase relationships of these rock systems (e.g., Inoue, 1994; Bose and Ganguly, 1995; Hirose, 1997; Kawamoto and Holloway, 1997; Schmidt and Poli, 1998; Ono, 1998) have been parameterized numerically and are incorporated into the model, especially concerning the maximum H_2O content (maximum $C_s^{H_2O}$ or $C_m^{H_2O}$) at a given $P-T$, including the melting conditions (Figs. 3 and 4).

The amount of H_2O that can be contained in the peridotite drastically changes corresponding to the stability of serpentine (Fig. 3a): at temperatures below 600–700 degrees C and pressures below 5 GPa, serpentine is stable and the peridotitic system can contain maximum ~8 wt.% H_2O in the solid phases. On the other hand, at temperatures above 600–700 degrees C, where serpentine and chlorite in the system are unstable, the maximum H_2O content in the solid phases (i.e., maximum $C_s^{H_2O}$) decreases: At pressures between 2.5 and 10 GPa, no major hydrous phase is know to exist for the peridotitic system above 600–700 degrees C, implying the maximum $C_s^{H_2O}$ is close to 0 wt.% in the $P-T$ range (Kawamoto and Holloway, 1997).

At pressures below 2.5 GPa and temperatures above 600–700 degrees C, amphibole is stable, and the

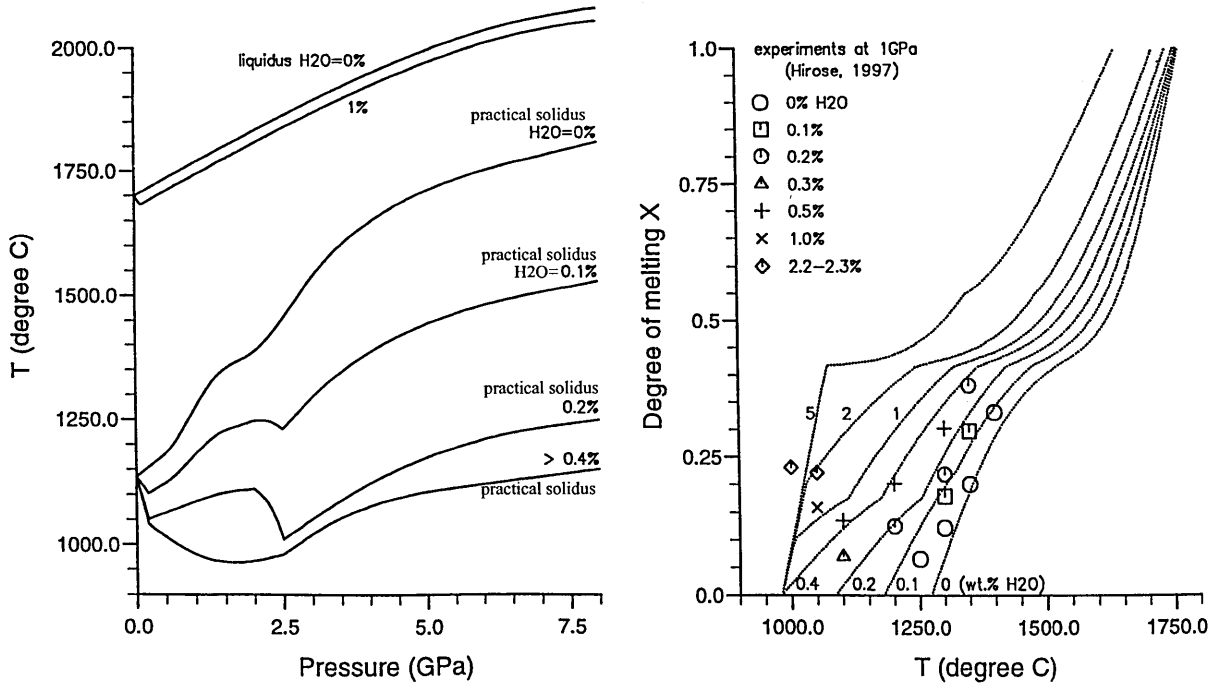

Fig. 4. Solidus and liquidus curves of peridotites for various H_2O contents (left), and the degree of melting as a function of the temperature and the H_2O content (after Iwamori (1998)).

maximum $C_s^{H_2O}$ is ~0.4 wt.% for peridotites (Schmidt and Poli, 1998). Amphibole is unstable above ~2.5 GPa, depending little on temperature. For these characteristics, dehydration of amphibole at 2.5 GPa has been thought to supply H_2O for melting beneath the volcanic front, and be responsible for the relatively constant depth of the Wadati-Benioff zone beneath the volcanic front in subduction zones (e.g., Tatsumi, 1989). However, (i) depth of the Wadati-Benioff zone below the volcanic front is not constant (e.g., ~3 GPa beneath northeast Japan, and ~5 GPa beneath central Japan); (ii) the amount of H_2O expelled from amphibole is small, and most of H_2O contained in the subducting plate is brought down to deeper by serpentine. These lines of evidences deny the conventional view that dehydration of amphibole leads to the formation of a volcanic front.

The maximum $C_s^{H_2O}$ of the subducting basaltic oceanic crust tends to decrease with an increase of pressure or temperature. Unlike the peridotitic system, the maximum $C_s^{H_2O}$ of the basaltic system changes nearly continuously as is shown in Fig. 3b, due to: (1) numerous reactions involving H_2O; and (2) effect of (solid) solution (Schmidt and Poli, 1998; Ono, 1998). Sedimentary rocks consisting of the top portion of the plate exhibit a similar trend in terms of the maximum $C_s^{H_2O}$ (Ono, 1998). Therefore, in this model, the maximum $C_s^{H_2O}$ of the subducting oceanic crust as a whole is represented as in Fig. 3b for the basaltic system.

The reaction that occurs at the highest temperature in Fig. 3a is melting of the unhydrous peridotite. As H_2O increases, the temperatures of the H_2O-undersaturated solidus defined by breakdown of amphibole ($\leq$2.5 GPa) and the practical solidus (>2.5 GPa) decrease. Note that the practical solidus temperature corresponds to the solidus temperature determined by high-pressure melting experiments, and indicates a temperature above which a detectable amount (more than a few percent) of silicate melt is formed. Utilizing the practical solidus for modeling of melting processes gives a reasonable approximation in terms of the energy balance, which is the major concern of this paper, although the incipient melt is crucial to the chemical behaviour of highly incompatible elements.

The amount of melt produced at a given pressure and temperature increases with an increasing amount of H_2O. Fig. 4 shows the results of parameterization for the $T-X$ (degree of melting) $-C_{H_2O}$ relationship of peridotite at 1 GPa. When the system is saturated with H_2O, addition of excess-H_2O

produces more melt at the onset of melting until the vapor phase (excess-H_2O) disappears. This behaviour is observed in the experiments of Hirose (1997), and is incorporated into the parameterization as shown in Fig. 4. Based on the parameterization, we are able to calculate the solidus and liquidus temperatures, $(\partial X/\partial T)_{P,C_{H_2O}}$, $(\partial X/\partial P)_{T,C_{H_2O}}$ and $(\partial X/\partial C_{H_2O})_{P,T}$ for the modeling (Iwamori, 1998).

According to the parameterized phase relationships, for a given set of temperature, pressure, and amount of H_2O in the local system (i.e., $C_b^{H_2O}$), we can calculate the amount of aqueous fluid, melt, solid, and the H_2O content in each phase. Each phase then flows and reacts, following equations (1) to (6), which in turn determines the temperature and $C_b^{H_2O}$ for the next time step.

This model is applied to the case with parameters that are appropriate for the Japan arcs and the boundary conditions shown in Fig. 1. The subducting plate is assumed to be a rigid slab with a constant subduction velocity and angle, which induces a corner flow in the mantle wedge due to drag force. Among the thermal boundary conditions shown in Fig. 1, the thermal structure of the subducting plate and the temperature profile given on the backarc boundary (left-hand side wall of the box of Fig. 1) are important. The former is constrained from the age of the subducting plate, and the latter is assumed to give a reasonable heat flux at the surface of the arc (Iwamori (1998) for the details). In the next chapter, based on the model results, the fluid processes beneath the Japan arcs (northeast Japan, central Japan, and southwest Japan) are discussed.

4. Results and discussion

4. 1 Northeast Japan

Northeast Japan is characterized by subduction of the Pacific plate nearly vertical to the Japan trench (Fig. 2), where a clear Wadati-Benioff zone and active volcanism with a well-defined volcanic chain are observed. Northeast Japan is one of the best studied area in terms of the seismic structures, including the tomographic image of the subducting plate and the mantle wedge (e.g., Zhao *et al.*, 1992), and is suitable for testing the model. Iwamori and Zhao (2000) applied the model in the previous chapter to northeast Japan to predict thermal structure, distribution of aqueous fluid and melt (Figs. 5a and 5b), and consequential seismic velocity structure (Figs. 5 c and 5d). They then compared the results with the P-wave tomographic images beneath the area (Figs. 5e to 5h).

For the subducted Pacific plate, the model calculation gives a relatively low temperature at the upper surface of the plate (e.g., ~600 degrees C at 200 km depth). In spite of the relatively cold environment, at depths greater than 30 km, H_2O is released from the subducting oceanic crusts, which is assumed to contain 6 wt.% H_2O initially (in amphibole, lawsonite, chlorite) before subduction. The style of aqueous fluid transportation is not well constained, depending on, e.g., the amount of fluid and wetting properties between the fluid and the crystals. Here we consider two cases: one assumes that the aqueous fluid migrates along the solid grain boundaries (porous flow), and achieves chemical equilibrium with the surrounding rocks during its migration (equilibrium model, Fig. 5a). Another assumes that the fluid is transported through sparsely distributed cracks (channel flow), partly violating chemical equilibrium (disequilibrium model, Fig. 5b).

In the equilibrium model for northeast Japan, H_2O expelled from the subducting slab forms serpentine in the mantle wedge just above the slab. Serpentine is brought down to a depth of ~150 km in the mantle wedge along the slab, where the temperature exceeds the stability fields of the minerals. The aqueous fluid expelled from these minerals ascends upwards due to density contrast. It reaches the core portion of the mantle wedge, where the temperature exceeds the hydrous solidus, and the melt is formed. In this case, dehydration and melting start from the backarc side, rather than beneath the volcanic front (the vertical line in Figs. 5a to 5g crosses the slab-wedge interface at a depth of 100 km, and corresponds to the approximate location of the volcanic front). In this model, the melt produced is not allowed to separate the residual solid, and is transported nearly horizontally with the flow of solid at a depth of ~80 km (Fig. 5a). In reality, the melt produced is expected to segregate upwards from the solid, resulting in a more dispersed distribution of melt, although the principal feature that dehydration and melting initiate in the backarc side remains the same.

The predicted distribution of temperature,

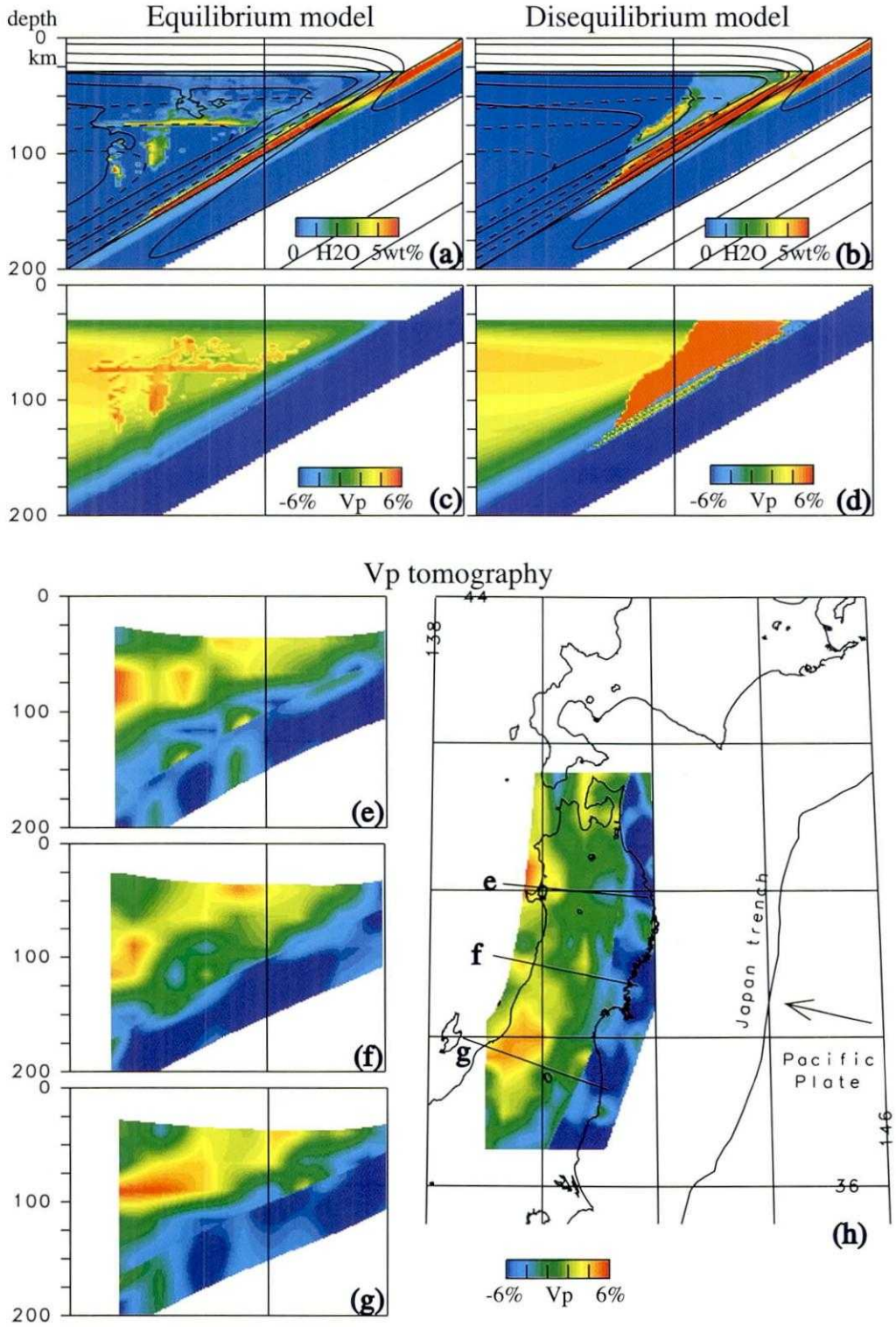

Fig. 5. (a, b) Distribution of H_2O predicted by a model for northeast Japan, and (c, d) Seismic (P-wave) velocity structure based on the fluid distribution predicted by the model for northeast Japan (after Iwamori and Zhao (2000)). The horizontal scale: vertical scale is 1: 1. See text for explanations of equilibrium (a, c) and disequilibrium model (b, d). The solid lines in (a, b) indicate the contours of temperature at intervals of 200 degrees C. The broken lines in (a, b) indicate the streamline. (e, f, g) Tomographic images for the P-wave velocity in across-arc sections and (h) a horizontal section at 80 km depth beneath northeast Japan, based on three-dimensional tomography (Zhao *et al.*, 1992; Iwamori and Zhao, 2000).

aqueous fluid, and melt is then used to predict the seismic velocities, using the thermodynamic relationships (e.g., Duffy and Anderson, 1989) and experimental results (Murase and Kushiro, 1977; Sato *et al.*, 1989). Assuming that the local melt fraction does not exceed 2 wt. % due to effective melt segregation, as stated above, the predicted P-wave velocity (V_P) beneath northeast Japan is shown in Fig. 5c. The result shows that V_P of the core portion (~75–100 km depth) of the mantle wedge is 4% lower, due to its higher temperature of ~1,250 degrees C, and is 6% lower where the melt is present such as beneath the backarc, compared to the ambient mantle at the same depth.

On the other hand, in the disequilibrium model that assumes channel flow and chemical isolation of a part of the aqueous fluid, H_2O expelled from the subducting slab is not entirely trapped by serpentine as it enters the mantle wedge, and a significant amount of aqueous fluid is supplied upwards from the subducting oceanic crust at depths shallower than 100 km (Fig. 5b). Consequently, a broad region beneath the forearc to volcanic front, where the depth of Wadati-Benioff zone is shallower than 100 km, is predicted to exhibit a significant decrease in seismic velocity (e.g., 6% decrease in V_P (Fig. 5d)).

Tomographic images (V_P) beneath northeast Japan are shown for representative across-arc 2-D sections and a horizontal section at a depth of 80 km in Figs. 5e to 5h (Zhao *et al.*, 1992; Iwamori and Zhao, 2000). The image shows that a remarkable low-V_P region of −6% exists beneath the backarc at a depth of 75–100 km, rather than beneath the volcanic front or forearc region. This observation, together with recent finer tomographic images of the same region for both P- and S-waves (Nakajima *et al.*, 2001), is well explained by the equilibrium model described above, in terms of both the location and the velocity. A recent seismological study also suggests the existence of a fluid-abundant region at a depth of 140–150 km around the interface between the subducted slab and the mantle wedge (Wyss *et al.*, 2001). This is again well explained by the equilibrium model (Figs. 5a and 5b), as serpentine breaks down to generate the aqueous fluid at a depth of ~150 km in the model. All these predictions and observations suggest that H_2O for the subduction zone magmatism is supplied from the backarc side by the aqueous fluid generated at ~150 km by the breakdown of serpentine (and chlorite), which is different from the conventional view.

4.2 Central Japan

Similar to northeast Japan, in central Japan (Figs. 2 and 6), the active volcanic chain exists corresponding to subduction of the old Pacific plate. While the volcanic chain in northeast Japan and the Izu-Ogasawara arc is located 80 to 150 km above the Wadati-Benioff zone of the subducted Pacific plate, it is located 200 to 300 km above the Wadati-Benioff zone in central Japan (Fig. 6), resulting in deflection of the volcanic chain towards the backarc side.

Iwamori (2000) modelled transportation of H_2O and melting beneath the central Japan for the cross-section A-B shown in Fig. 6, based on equations (1) to (6) and the plate configuration deduced from the seismic studies (Ishida, 1992). In the cross-section, the Philippine sea plate should have a velocity component perpendicular to the cross-section. However, the motion of the Philippine sea plate is much slower than that of the Pacific plate, so the subducted Philippine sea plate is modelled as a stagnant block in the mantle wedge. In this case, a hot mantle material from the backarc is prevented from flowing into the corner region as shown by the stream line (Fig. 7), resulting in a slow thermal recovery of the subducting Pacific plate (e.g., 370 degrees C at a depth of 100 km, 550 degrees C at 200 km, whereas 490 and 610 degrees C for northeast Japan). Consequently, the dehydration reactions of serpentine are shifted deeper, resulting in melting far from the trench (Fig. 7). The model result also indicates that H_2O is not entirely released from the solid phase even after dehydration of serpentine and chlorite, as phase-A is stable at the pressure and can bring down a significant amount of H_2O to a depth greater than 300 km.

4. 3 Southwest Japan

In contrast with the relatively cold environment in northeast and central Japan, subduction of the young Shikoku basin (27 to 15 Ma, Fig. 2) significantly affects the fluid processes beneath Shikoku, Chugoku, and northern Kyushu in southwest Japan. As has been clarified by the discussion so far, the young subducted slab causes dehydration reactions at depths shallower than beneath northeast and central Japan. Figure 8a shows the model prediction for such a case with the subduction of a

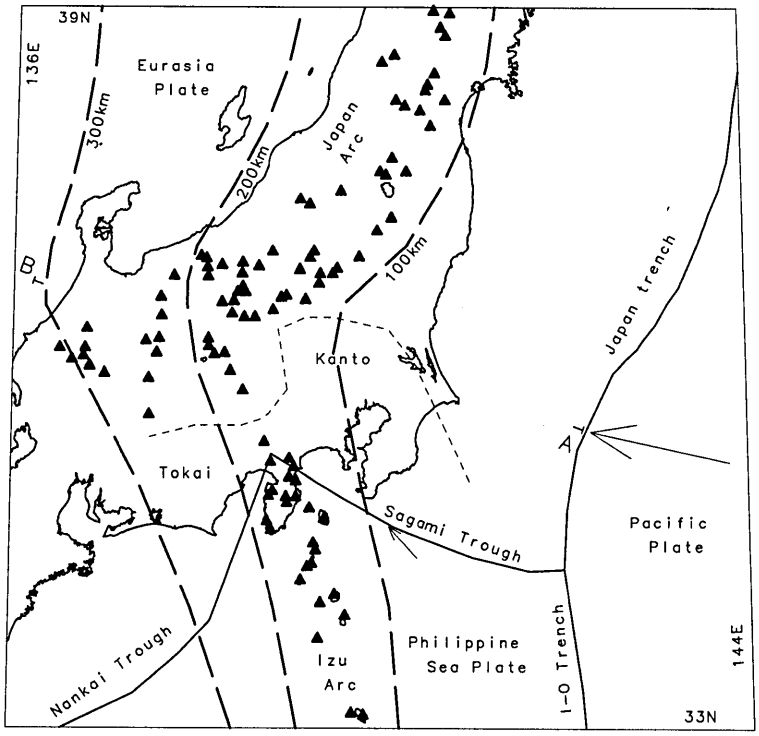

Fig. 6. Distribution of volcanoes (solid triangle), depth contours of the Wadati-Benioff zone of the subducted Pacific plate (thick dashed line), and the leading edge of the subducted Philippine Sea plate (thin dashed line) after Iwamori (2000).

young (20 Ma) slab, showing that the aqueous fluid and the melt are distributed beneath the volcanic front to forearc region, rather than beneath the backarc.

The tomographic image (V_P) beneath northern Kyushu, across-arc section through Kuju volcano, is presented in Fig. 8b (Zhao *et al.*, 2000). The image shows a low V_P region extending beneath the Kuju volcano (volcanic front) to the forearc region. Although the model result in Fig. 8a is not converted to the seismic velocity structure, the distribution pattern of the fluid in the model coincides well with the low V_P region in the tomographic image. Therefore, the aqueous fluid is mainly present beneath the volcanic front to forearc regions in northern Kyushu, due to subduction of the warm Shikoku basin (Fig. 9 c). This is also supported by looking at the tomographic image and the seismicity in central to southern Kyushu (Zhao *et al.*, 2000), where a relatively cold plate subducts (older than 50 Ma, Fig. 2): the low-V_P region and the dense seismicity in the forearc region disappears. Instead, a low-V_P region appears beneath the volcanic front to backarc side (Zhao *et al.*, 2000). Since the other subduction parameters such as subduction velocity and angle are similar for northern and southern Kyushu, it is concluded that the age of the subducting plate controls the fluid processes in the region.

5. Summary and conclusions

Numerical models for the transportation of H_2O and melting beneath the Japanese arcs are presented, in which generation and migration of aqueous fluid, its interaction with the convecting solid, and melting are considered, based on phase relationships. Comparisons between the model results and observations (seismic structures and distribution of volcanoes) in northeast, central, and southwest Japan reveal the following points:

(1) An aqueous fluid released from the subducting plate forms serpentine in the mantle wedge just above the subducting plate, maintaining chemical equilibrium during migration. Most of the H_2O is brought down to a depth where serpentine and chlorite break down. This depth depends on the thermal structure of the slab, which is controlled mainly by

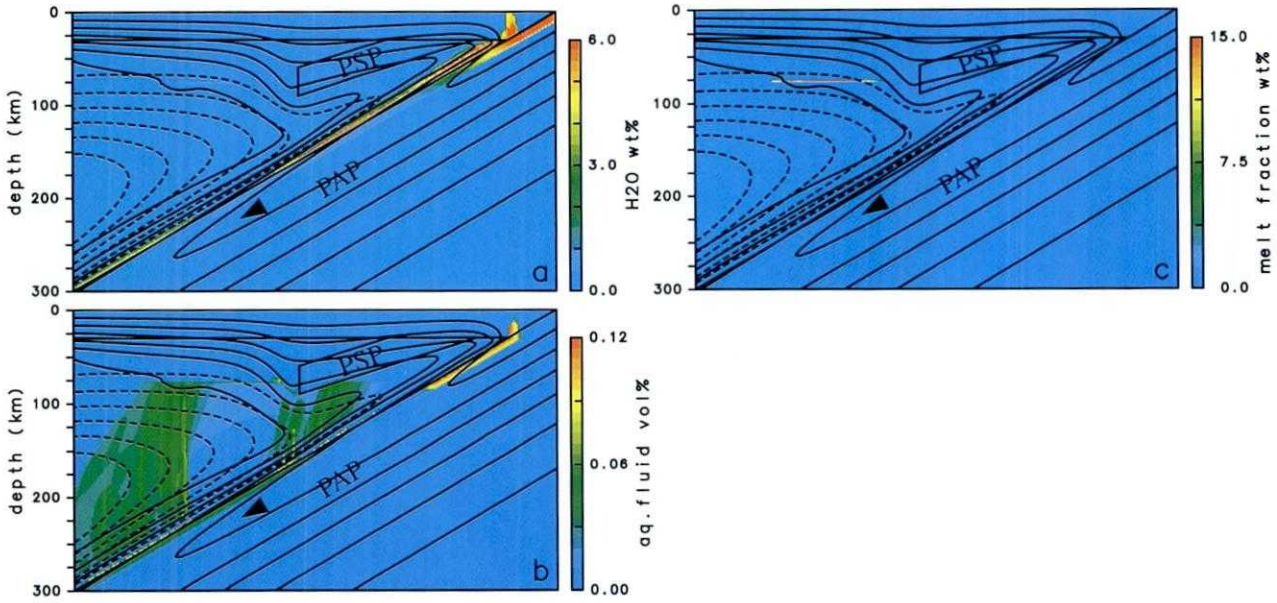

Fig. 7. A model of transportation of H_2O and melting beneath central Japan. The two-dimensional section corresponds to the across-arc section A-B shown in Fig. 6. PAP and PHP denote the Philippine Sea plate and the Pacific plate, respectively. The solid lines indicate the contours of temperature at intervals of 200 degrees C. The broken lines indicate the streamline.

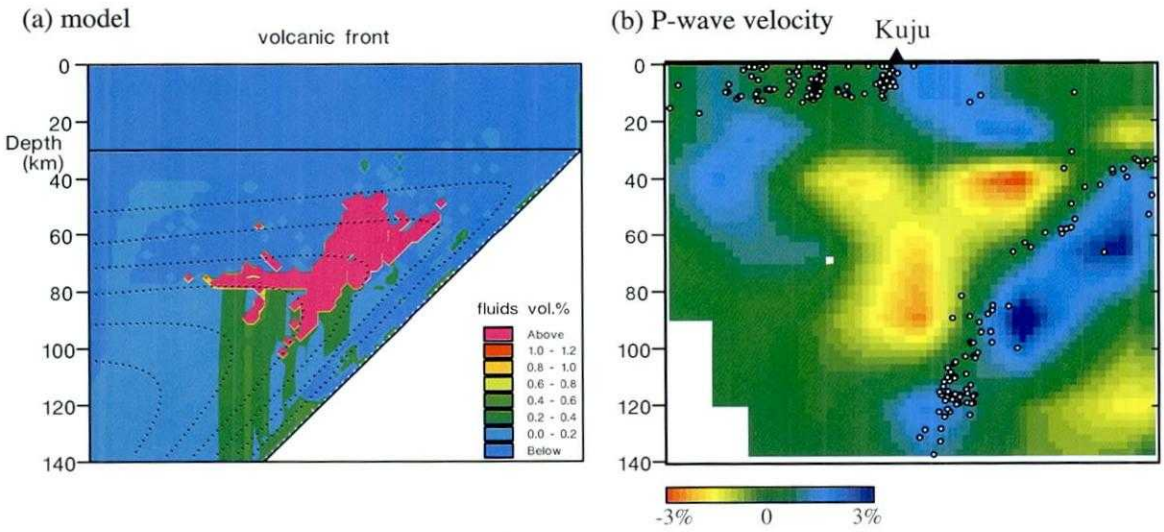

Fig. 8. (a) Distribution of fluids (aqueous fluid and melt) beneath southwest Japan (northern Kyushu), predicted by the model, and (b) P-wave velocity section beneath northern Kyushu based on three-dimensional tomography (after Zhao *et al.* (2000)). The broken lines in (a) indicate the streamlines of solid.

the age of the subducting plate and subduction velocity. If the subduction velocity is the same, the dehydration depth is greater for the older plate: ~ 150 km for subduction of the Pacific plate (130 Ma old) in northeast Japan (Fig. 9a), and less than 100 km for subduction of the Shikoku basin (~20 Ma old, Fig. 9 c). Considering that the Pacific plate is one of the oldest plates in the world, in most of the subduction zones, dehydration of the oceanic crusts and the overlying mantle wedge (the serpentinite layer) is completed at depths shallower than 200 km. The aqueous fluid generated at these depths ascends to

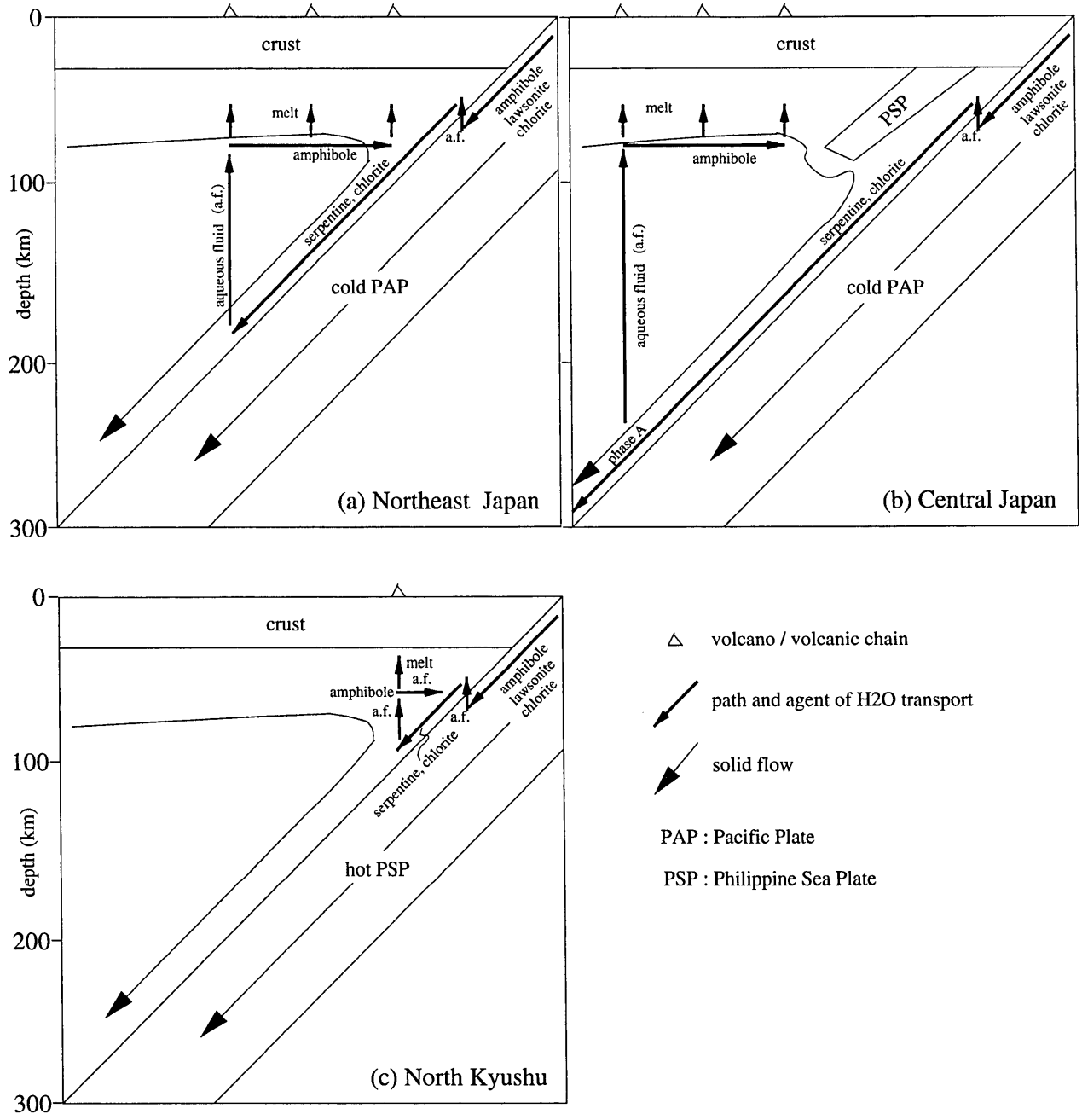

Fig. 9. Schematic figure showing transportation of H_2O and its host phases.

cause melting in the core portion of the mantle wedge. The predicted position and the amount of the aqueous fluid and melt can explain well seismic tomographic images and the spatial variation of the earthquake size-frequency relationship. (2) Beneath central Japan, the subducted Philippine sea plate overlapping the subducted Pacific plate causes a slow thermal recovery of the latter, resulting in dehydration and melting far from the trench (Fig. 9b). Consequently, the volcanic chain in the region deflects towards the backarc side. In this case, as an exception to what was described in (1), H_2O is brought down to depth greater than 300 km by phase-A, even after breakdown of serpentine.

Acknowledgments

The author thanks J. Kasahara, D. McKenzie, C. Richardson, Y. Takei, D. Zhao for their discussions and assistance.

References

Bose, K. and J. Ganguly, 1995, Experimental and theoretical studies of the stabilities of talc, antigorite and phase A at high pressures with applications to subduction processes, *Earth Planet. Sci. Lett.*, **136**, 109-121.

DeMets, C., R.G. Gordon, D.F. Argus and S. Stein, 1990, Current plate motions, *Geophys. J. Int.*, **101**, 425-478.

Duffy, T.S. and D.L. Anderson, 1989, Seismic velocities in mantle minerals and the mineralogy of the upper mantle, *J. Geophys. Res.* **94**, 1895-1912.

Hirose, K., 1997, Melting experiments on lherzolite KLB-1 under hydrous conditions and generation of high-magnesian andesitic melts, *Geology*, **25**, 42-44.

Inoue, T., 1994, Effect of water on melting phase relations and melt composition in the system Mg_2SiO_4-Mg SiO_3-H_2O up to 15 GPa, Phys, *Earth Planet. Inter.*, **85**, 237-263.

Ishida, M., 1992, Geometry and relative motion of the Philippine Sea plate and Pacific plate beneath the Kanto-Tokai District, Japan, *J. Geophys. Res.*, **97**, 489-513.

Iwamori, H., 1991, Zonal structure of Cenozoic basalts related to mantle upwelling in southwest Japan, *J. Geophys. Res.*, **96**, 6157-6170.

Iwamori, H., 1992, Degree of melting and source composition of Cenozoic basalts in southwest Japan: evidence for mantle upwelling by flux melting, *J. Geophys. Res.*, **97**, 10983-10995.

Iwamori, H., 1998, Transportation of H_2O and melting in subduction zones, *Earth Planet. Sci. Lett.*, **160**, 65-80.

Iwamori, H., 2001, Deep subduction of H_2O and deflection of volcanic chain towards backarc near triple junction due to lower temperature, *Earth Planet. Sci. Lett.*, **181**, 41-46.

Iwamori, H. and D. Zhao, 2000, Melting and seismic structure beneath the northeast Japan arc, *Geophys. Res. Lett.*, **27**, **425-428.**

Nakajima, J., T. Matsuzawa, A. Hasegawa and D. Zhao, 2001, Three-dimensional structure of Vp, Vs and Vp/Vs beneath northeastern Japan: implications for arc magmatism and fluids, *J. Geophys. Res.*, **106**, 21843-21857.

Kawamoto, T. and Holloway, J., 1997, Melting temperature and partial melt chemistry of H_2O-saturated mantle peridotite to 11 gigapascals, *Science*, **276**, 240-243.

Kondo, H., K. Kaneko and K. Tanaka, 1998, Characterization of spatial and temporal distribution of volcanoes since 14Ma in the Northeast Japan arc, *Bull. Volcanol. Soc. Jpn.*, **43**, 173-180.

McKenzie, D., 1984, The generation and compaction of partially molten rock, *J. Petrol.*, **25**, 713-765.

Murase, T. and I. Kushiro, 1977, Compressional wave velocity in partially molten peridotite at high pressures. Carnegie Inst. Wash. Year Book **78**, 559-562.

Nakanishi, I., 1980, Precursors to ScS phases and dipping interface in the upper mantle beneath southwestern Japan., *Tectonophys.*, **69**, 1-35.

Okino, K., Y. Shimakawa and S. Nagaoka, 1994, Evolution of the Shikoku Basin, *J. Geomag. Geoelectr.*, **46**, 463-479.

Ono, S., 1998, Stability limits of hydrous minerals in sediment and mid-ocean ridge basalt compositions: implications for water transport in subduction zones, *J. Geophys. Res.*, **103**, 18253-18267.

Sato, H., I.S. Sacks and T. Murase, 1989, The use of laboratory velocity data for estimating temperature and partial melt fraction in the low velocity zone: comparison with heat flow and electrical conductivity studies, *J. Geophys. Res.* **95**, 5689-5704.

Schmidt, M. and S. Poli, 1998, Experimentally based water budgets for dehydrating slabs and consequences for arc magma generation, *Earth Planet. Sci. Lett.*, **163**, 361-379.

Seno, T., S. Stein and A.E. Gripp, 1993, A model for the motion of the Philippine sea plate consitent with Nuvel-1 and geological data, *J. Geophys. Res.*, **98**, 17941-17948.

Tatsumi, Y., 1989, Migration of fluid phases and genesis of basalt magmas in subduction zones, *J. Geophys. Res.*, **94**, 4697-4707.

Tokuyama, H., 1995, Origin and development of the Philippine Sea, In: Geology and Geophysics of the Philippine Sea, eds. H. Tokuyama, S.A. Shcheka, N. Isezaki et al., Terrapub, pp. 155-163.

Whitford-Stark, J.L., 1987, A survey of Cenozoic volcanism on mainland Asia, Geol. Soc. Am. Spec. Paper 213, 74 pp.

Wyss, M., A. Hasegawa and J. Nakajima, 2001, Source and path of magma for volcanoes in the subduction zone of northeastern Japan, *Geophys. Res. Lett.*, **28**, 1819-1822.

Yamazaki, F., T. Ooida and H. Aoki, 1989, Subduction of the Philippine Sea plate beneath the Tokai area, central Japan, *J. Earth Sci. Nagoya Univ.*, **36**, 15-26.

Yoshii, K., 1979, Compilation of the geophysical data around the Japan arcs (I) (in Japanese), *Bull. Earthquake Res. Inst. Univ. Tokyo*, **54**, 75-117.

Zhao, D., A. Hasegawa and S. Horiuchi, 1992, Tomographic imaging of P and S wave velocity structure beneath northeastern Japan, *J. Geophys. Res.*, **97**, 19909-19928.

Zhao, D. and A. Hasegawa, 1993, P wave tomographic imaging of the crust and upper mantle beneath the Japan islands, *J. Geophys. Res.*, **98**, 4333-4353.).

Zhao, D., K. Asamori and H. Iwamori, 2000, Seismic structure and magmatism of the young Kyushu subduction zone, *Geophys. Res. Lett.*, **27**, 2057-2060.

(Received July 2, 2001)
(Accepted October 4, 2001)